Electric-field-induced modulation of the anomalous Hall effect in a heterostructured itinerant ferromagnet $SrRuO_3$

Hayato Mizuno,[1] Kihiro T. Yamada,[1] Daisuke Kan,[1,*] Takahiro Moriyama,[1] Yuichi Shimakawa,[1,2] and Teruo Ono[1,3,†]

[1]*Institute for Chemical Research, Kyoto University, Uji, Kyoto 611-0011, Japan*
[2]*Integrated Research Consortium on Chemical Sciences, Uji, Kyoto 611-0011, Japan*
[3]*Center for Spintronics Research Network (CSRN), Graduate School of Engineering Science, Osaka University, Toyonaka, Osaka 560-8531, Japan*

(Received 12 October 2017; revised manuscript received 1 December 2017; published 15 December 2017)

We fabricated electric-field-effect transistor structures with a channel layer of an itinerant ferromagnet $SrRuO_3$ (SRO) heterostructured with a cap layer of $BaTiO_3$ and investigated the electric field effects on the anomalous Hall effect (AHE) in SRO. We show that by applying positive and negative gate voltages (V_G), the anomalous Hall conductivity in the heterostructured SRO increases and decreases, respectively, regardless of its sign, while no change in the magnetic easy axis direction is observed. The results indicate that the observed V_G-induced modulations of the AHE do not simply originate from changes in the magnetization and magnetic anisotropy and indicate that V_G-induced changes in an integral of the Berry curvature over the filled electronic states play a key role in the observed electric field effects on the AHE in SRO. We also found that V_G-induced modulations on the AHE are negligibly small for transistor structures with a SRO channel having no BTO cap layer. This implies that the cap-layer-induced modifications in the Ru-O-Ru bond angles in the channel affect the Berry phase, enhancing the electric field effects on the AHE in SRO.

DOI: 10.1103/PhysRevB.96.214422

Berry curvature in conduction bands is a key concept in modern condensed matter physics and plays decisive roles in a wide variety of emergent phenomena in solids [1]. For magnetic materials, conduction electrons coupled with magnetization can sense fictitious magnetic fields because of Berry curvature, leading to intriguing magnetotransport phenomena such as the anomalous Hall effect (AHE) in ferromagnets [2,3,4,5,6] and antiferromagnets [7,8] and the topological Hall effect [9,10]. In fact, the intrinsic anomalous Hall conductivity $\sigma_{AHE} = \rho_{AHE}/(\rho_{xx}{}^2 + \rho_{AHE}{}^2)$ (ρ_{xx}: longitudinal electrical resistivity, ρ_{AHE}: anomalous Hall resistivity) is known to be proportional to the integral of the Berry curvature over the filled electronic states [2]. An important implication is that the integrated Berry curvature can be modulated by electrically changing the electron fillings in the conduction bands, allowing for electrically controlling the AHE in ferromagnets.

A perovskite, strontium ruthenate $SrRuO_3$ (SRO), is known to be an itinerant ferromagnet and has attracted a great deal of attention [11,12,13]. It has been revealed that the AHE of this oxide exhibits unique behavior [14,15] not seen in conventional ferromagnetic metals. The magnitude and sign of the anomalous Hall resistivity ρ_{AHE} nonmonotonically change with temperature, while the magnetization changes monotonically. Theoretical investigations [14,16] have demonstrated that SRO exhibits multiple band crossings consisting of different bands around the Fermi level E_F. Such band crossings act either as a source or a sink of Berry curvature and are regarded as monopoles of the emergent magnetic field in momentum space. Although the exact mechanism of the AHE of SRO remains under debate [17,18], the Berry curvature contributes dominantly to the AHE of SRO and the experimentally observed behavior of the ρ_{AHE} of SRO can be attributed to the change in the integrated Berry curvature associated with the temperature-induced modulations of electron distributions around E_F. Given that applying bias voltages (or gate voltages) can also affect the electron distributions around E_F or the Fermi level position, this raises the possibility of electrically modulating the AHE in SRO.

In this study, we investigate the electric-field-induced effects on the AHE of heterostructured SRO. We found that by gating SRO, both the magnitude and sign of σ_{AHE} can be modulated. Our observations, including no electric-field-induced effects on the magnetic anisotropy of SRO, indicate that the gate voltage (V_G) induced modulations of σ_{AHE} do not simply originate from changes in the magnetization and the anisotropy, highlighting the significance of the Berry curvature for the electric-field-induced effects on σ_{AHE} in SRO.

An SRO-based epitaxial channel layer for field-effect transistor structures was grown on (110) $GdScO_3$ (GSO) substrates by pulsed laser deposition (PLD). A 4-nm-thick (~10 monolayers) SRO layer was deposited at a substrate temperature of 700 °C under an oxygen partial pressure of 100 mTorr. A 1-nm-thick (~4 monolayers) cap layer of $BaTiO_3$ (BTO) was successively deposited at 700 °C under 30 mTorr without breaking the vacuum of the PLD chamber. The fabricated BTO/SRO/GSO heterostructure was cooled to room temperature under 100 mTorr of oxygen pressure. The epitaxial growth of the channel layer was confirmed from the x-ray $2\theta/\theta$ diffraction profile in Fig. 1(a). While the diffraction intensities from the BTO layer were too weak to detect, the $(220)_{ortho}$ reflection from the SRO layer was clearly observed, indicating $(110)_{ortho}$-oriented growth of the SRO layer on the substrate. The x-ray reciprocal space mapping measurements [19] show that the capped SRO layer is coherently grown on the substrate and has a monoclinic structure whose magnetic easy axis is parallel to its $[100]_{ortho}$ direction [20,21].

*dkan@scl.kyoto-u.ac.jp
†ono@scl.kyoto-u.ac.jp

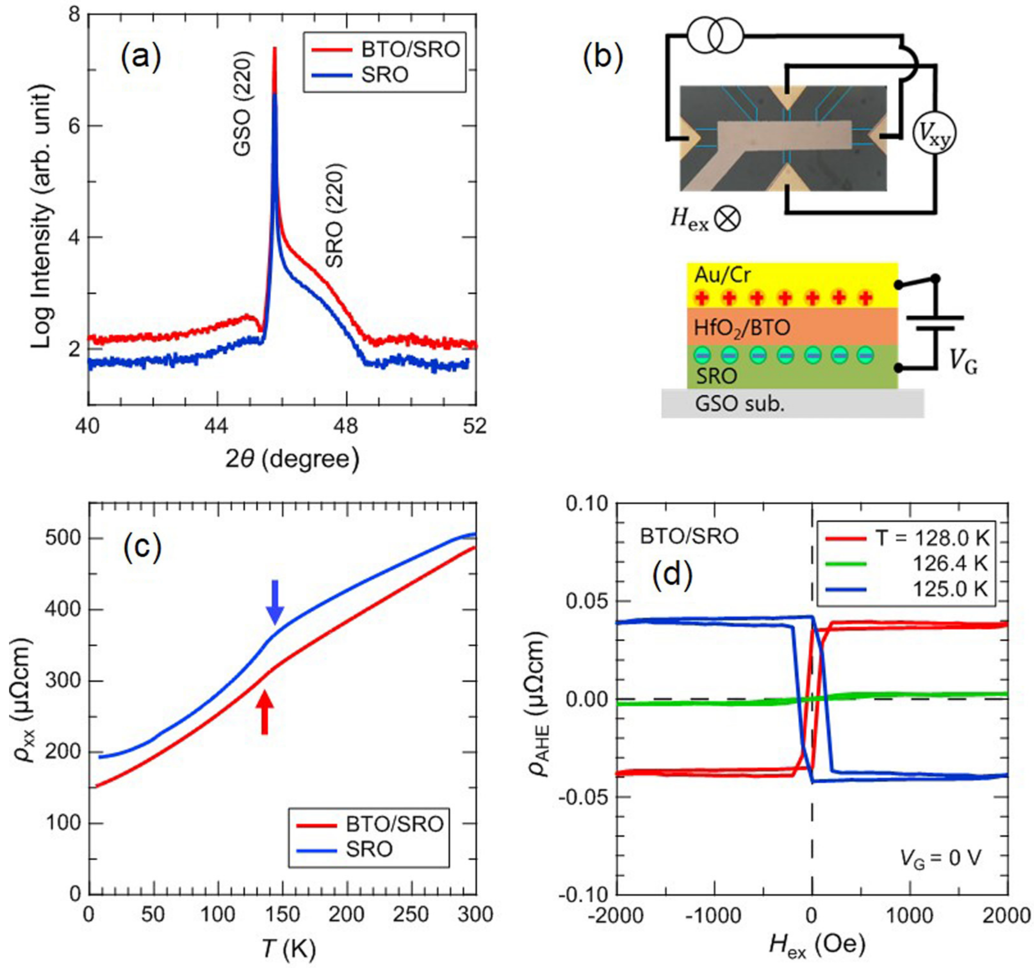

FIG. 1. (a) X-ray $2\theta/\theta$ profiles of the $BaTiO_3$(BTO)/$SrRuO_3$(SRO)/$GdScO_3$(GSO) and SRO/GSO heterostructures. (b) Optical image and schematic of our fabricated field-effect transistor structures. (c) Temperature dependence of the electrical resistivity ρ_{xx} for the BTO/SRO and SRO channels in the transistor structures. The data were recorded without the application of V_G ($V_G = 0$ V). The ferromagnetic transition temperatures (T_C) indicated by arrows in the graph (135 K for the BTO/SRO channel and 142 K for the SRO channel) were determined from the temperature derivative of each ρ_{xx} - T curve. (d) Magnetic field dependence of the anomalous Hall resistivity ρ_{AHE} for the BTO/SRO channel under $V_G = 0$. The data were recorded at 128.0 K (red), 126.4 K (green), and 125.0 K (blue).

To fabricate field-effect transistor structures, the BTO/SRO epitaxial layer (hereafter referred to as the BTO/SRO channel) was patterned into a 30-μm-wide Hall bar by conventional photolithography and Ar ion milling. A 50-nm-thick gate insulating layer of HfO_2 was then deposited on the entire sample surface by atomic layer deposition. To gate the BTO/SRO channel, gate electrodes of Au(40 nm)/Cr(5 nm) layers were thermally evaporated on the HfO_2 layers with the channel underneath. An optical image of our fabricated transistor structure is presented in Fig. 1(b). In order to see how the BTO cap layer affects the gate-voltage-induced effects of the channel, we also fabricated transistor structures with a SRO channel having no BTO cap layer (referred to as the SRO channel) and a HfO_2 gate insulator layer directly deposited on top of the channel. All transport measurements in this study were carried out by applying the excitation current of 200 μA along the channels. It was also confirmed that upon the application of the gate voltages, the leak current through the gate insulator layer was less than 100 pA.

Figure 1(c) shows the temperature dependence of the longitudinal electrical resistivity ρ_{xx} of the BTO/SRO and SRO channels in the transistor structures. Both channels exhibit metallic conduction down to low temperatures and undergo ferromagnetic transitions, which are seen as humps in the ρ_{xx} - T curves. The ferromagnetic transition temperature (T_C) is found be about 135 K in the BTO/SRO channel and about 142 K in the SRO channel. To evaluate the AHE in the channels, we measured the Hall resistivity ρ_{xy} by sweeping the magnetic field H_{ex} normal to the sample surface. Asymmetric components in ρ_{xy}, which originate from misalignments of the samples, were corrected by taking the difference between the ρ_{xy} measured at the magnetic fields of $+H_{ex}$ and $-H_{ex}$ and normalizing the readings: $\rho_{xy}(+H_{ex}) = [\rho_{xy}(+H_{ex}) - \rho_{xy}(-H_{ex})]/2$. The ordinary part of ρ_{xy} was determined by linearly fitting ρ_{xy} in the higher magnetic field region. We note that the carrier density of the SRO layer determined from the ordinary part of ρ_{xy} is on the order of $10^{22}\,cm^{-3}$. The anomalous part of ρ_{xy}, ρ_{AHE}, was extracted by subtracting the ordinary part from the measured signal. Figure 1(d) shows the

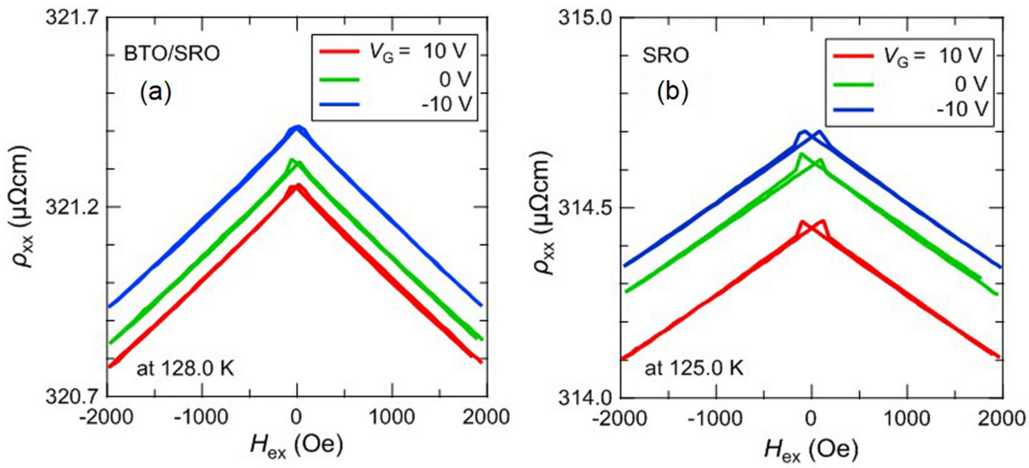

FIG. 2. Magnetic field dependence of the electrical resistivity ρ_{xx} for the transistor structures with the (a) BTO/SRO and (b) SRO channels under various V_G. The data were recorded at 128.0 K and 125.0 K for the transistor structures with the BTO/SRO and SRO channels, respectively.

magnetic field dependence of ρ_{AHE} for the BTO/SRO channel under zero gate voltage ($V_G = 0$ V) and at 125.0 K, 126.4 K, and 128.0 K. The curves at 125.0 K and 128.0 K exhibit square-shaped hysteresis because of the H_{ex}-induced reversal of the magnetization, confirming that the magnetization of the SRO layer possesses an out-of-plane component. At 126.4 K (defined as T_S), ρ_{AHE} becomes negligibly small and the sign of ρ_{AHE} in the positive H_{ex} is also found to change from positive to negative with decreasing temperature from T_C through T_S. This behavior is also confirmed from the temperature dependence of the anomalous Hall conductivity σ_{AHE} [22]. In addition to the change in the sign of σ_{AHE}, the magnitude of σ_{AHE} nonmonotonically changes with temperature. The observed behavior of AHE agrees with previous reports [11,14,15], highlighting the significance of the Berry curvature on the AHE of the SRO layer. We note that the AHE of the SRO channel having no the BTO cap layer whose T_S is 123.2 K exhibits similar behavior to those seen for the BTO/SRO channel [22].

The V_G-induced effects on the transport properties of the channels were evaluated by measuring the magnetic field H_{ex} dependence of ρ_{xx} and ρ_{AHE} under various V_G. Figures 2(a) and 2(b) show the H_{ex} dependence of ρ_{xx} for the transistor structures with the BTO/SRO and SRO channels under $V_G = +10$ V, 0 V, and -10 V. We found that ρ_{xx} of both channels are modulated by applying V_G. Under $V_G = 0$ V, both channels exhibit negative magnetoresistance whose magnitudes are about 0.1% at H_{ex} of 2000 Oe. In our device configuration, by applying positive and negative V_G, the accumulation and depletion of electron carriers with an order of about 10^{18} cm^{-3} into the channels is expected, respectively. The expected carrier density was calculated by assuming that the HfO_2 gate insulating layer has a dielectric constant of 20 and is under $V_G = 10$ V. As we expected, applying V_G of $+10$ V and -10 V respectively decreases and increases ρ_{xx} by 0.04% from the value under $V_G = 0$ V, while the magnitude of the magnetoresistance under the application of V_G remains unchanged. The results indicate that regardless of the capping for the SRO channels, the channels are electrostatically accumulated and depleted through the application of V_G. Given that the carrier mobility is unchanged against the application of V_G, rough estimations from the V_G-induced changes in ρ_{xx} indicate that the modulated carrier density in SRO is approximately 6×10^{18} cm^{-3}, which is in close agreement with the modulated carrier number that is expected based on the dielectric constant of the gate insulator. We also see that ρ_{xx} of the channels change back to the value close to the original value under $V_G = 0$ V when V_G is set back to 0 V [23]. This indicates that contributions of possible ferroelectricity [24] in the BTO cap layer to the observed V_G-induced changes in ρ_{xx} are negligibly small.

Figure 3 compares the V_G-induced changes in the H_{ex} dependence in ρ_{AHE} for the transistor structures with the BTO/SRO and SRO channels. The dependence in the ρ_{AHE} - H_{ex} curves was measured at temperatures above, at, and below T_S for each transistor structure. We found that the electric field effects on the AHE in the channels strongly depend on the capping of the channels. The magnitude and sign of ρ_{AHE} in the capped channel (BTO/SRO) are modulated by applying V_G, while the coercive fields in the ρ_{AHE} - H_{ex} curves exhibit no change with V_G [Figs. 3(a)–3(c)]. In contrast, the curves for the SRO channel in Figs. 3(d)–3(e) exhibit no (or negligibly small) V_G-induced changes in ρ_{AHE}. It should be emphasized that the application of V_G results in electrostatic accumulations and depletions of electron carriers with an order of 10^{18} cm^{-3} into the channels (Fig. 2), although no apparent V_G-induced changes in the ordinary part of ρ_{xy} are seen. This highlights that the BTO cap layer plays a decisive role in the V_G-induced modulation of the AHE.

Our observations of the BTO/SRO channel in Figs. 3(a)–3(c) indicate that at 128.0 K (above T_S), an increase and decrease in ρ_{AHE} are respectively induced by positive and negative V_G while the sign of ρ_{AHE} remains positive [Fig. 3(a)]. As the temperature decreases to T_S (126.4 K), at which the ρ_{AHE} is negligibly small [Fig. 3(b)], positive and negative ρ_{AHE} are induced by positive and negative V_G, respectively, demonstrating that V_G controls the sign of ρ_{AHE} at this temperature. With a further decrease in temperature to 125.0 K [below T_S in Fig. 3(c)], at which the sign of ρ_{AHE} turns negative, a V_G-induced increase in ρ_{AHE} is still seen. These V_G-induced changes in ρ_{AHE} have not been observed in previous studies

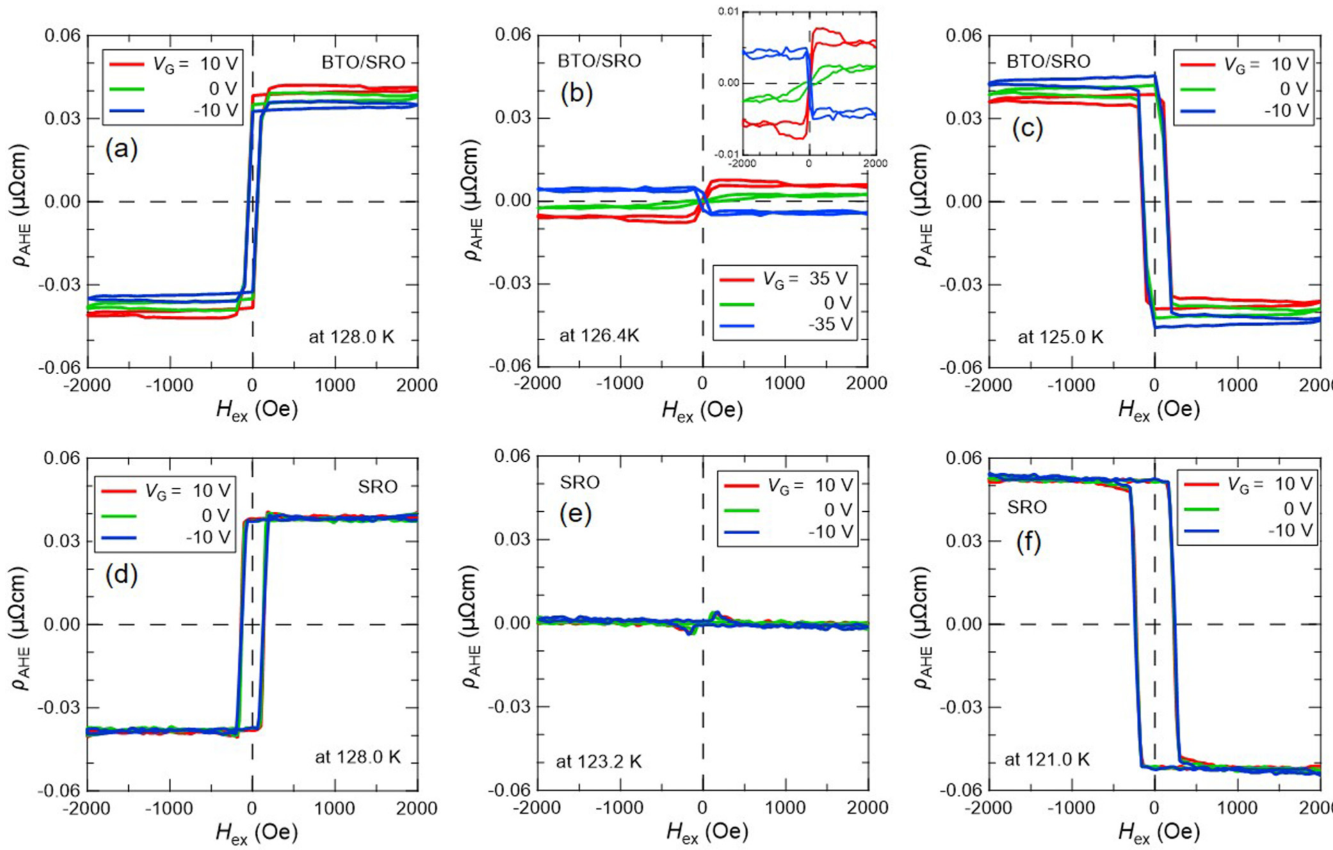

FIG. 3. Magnetic field dependence of ρ_{AHE} of the (a)–(c) BTO/SRO and (d)–(e) SRO channels under various V_{G}. The data were recorded at temperatures (a), (d) above; (b), (e) at; and (c), (f) below T_{S}. T_{S} is defined as the temperature at which ρ_{AHE} becomes zero (or negligibly small), and is 126.4 K for the BTO/SRO channel and 123.2 K for the SRO channel. In (b), the inset shows the vertically expanded view of the curves in the curves on Fig. 3(b).

on the electric field effects on atomically thin SRO films [25] as well as conventional ferromagnetic metal thin films and artificial structures [26,27,28]. Our observations point to the conclusion that the anomalous Hall conductivity σ_{AHE} ($\sim\rho_{\text{AHE}}/\rho_{xx}^2$) increases and decreases by applying positive and negative V_{G}, respectively. Figure 4 shows the V_{G} dependence of σ_{AHE} for the BTO/SRO channel at 128.0 K, 126.4 K, and 125.0 K. For all temperatures, a linear relationship between ρ_{AHE} and V_{G} is seen regardless of the sign of σ_{AHE}. We note that an increase in σ_{xy} is also seen when raising the temperature under $V_{\text{G}} = 0$ V (Figs. 1(d) and Ref. [22]). Given that the magnetization of SRO decreases monotonically with the increase in temperature [11,29], the observed V_{G}-induced change in σ_{AHE} is contrary to what is expected from the temperature-induced magnetization change. This behavior implies that the V_{G}-induced change in the carrier density is too small to modulate the magnetization and that the observed V_{G}-induced change in σ_{AHE} does not simply originate from the magnitude change of the magnetization. Our observations are in stark contrast to the previously observed electric-

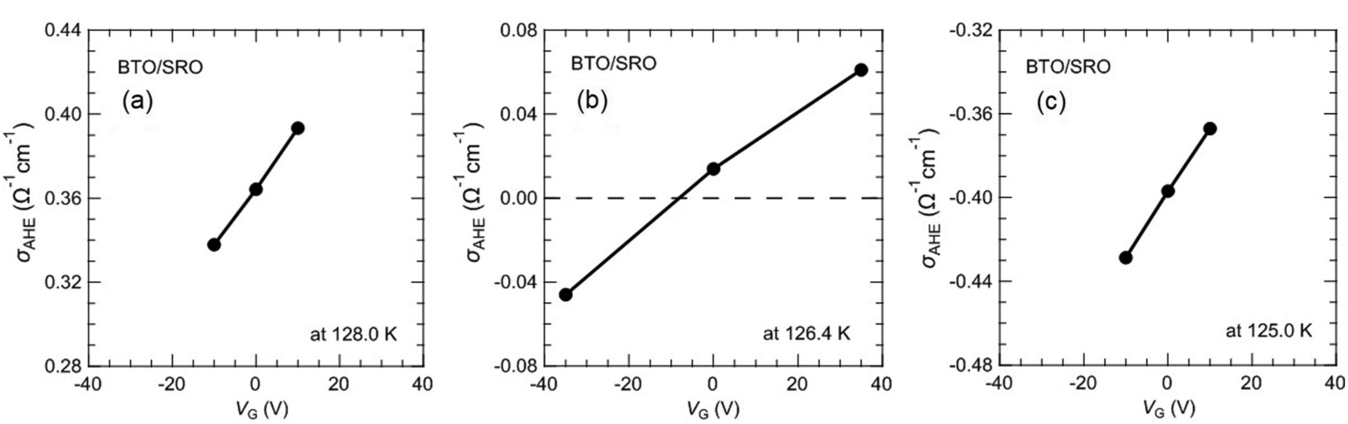

FIG. 4. V_{G} dependence of the anomalous Hall conductivity σ_{AHE} ($\sim\rho_{\text{AHE}}/\rho_{xx}^2$) for the BTO/SRO channel (a) above, (b) at, and (c) below T_{S}.

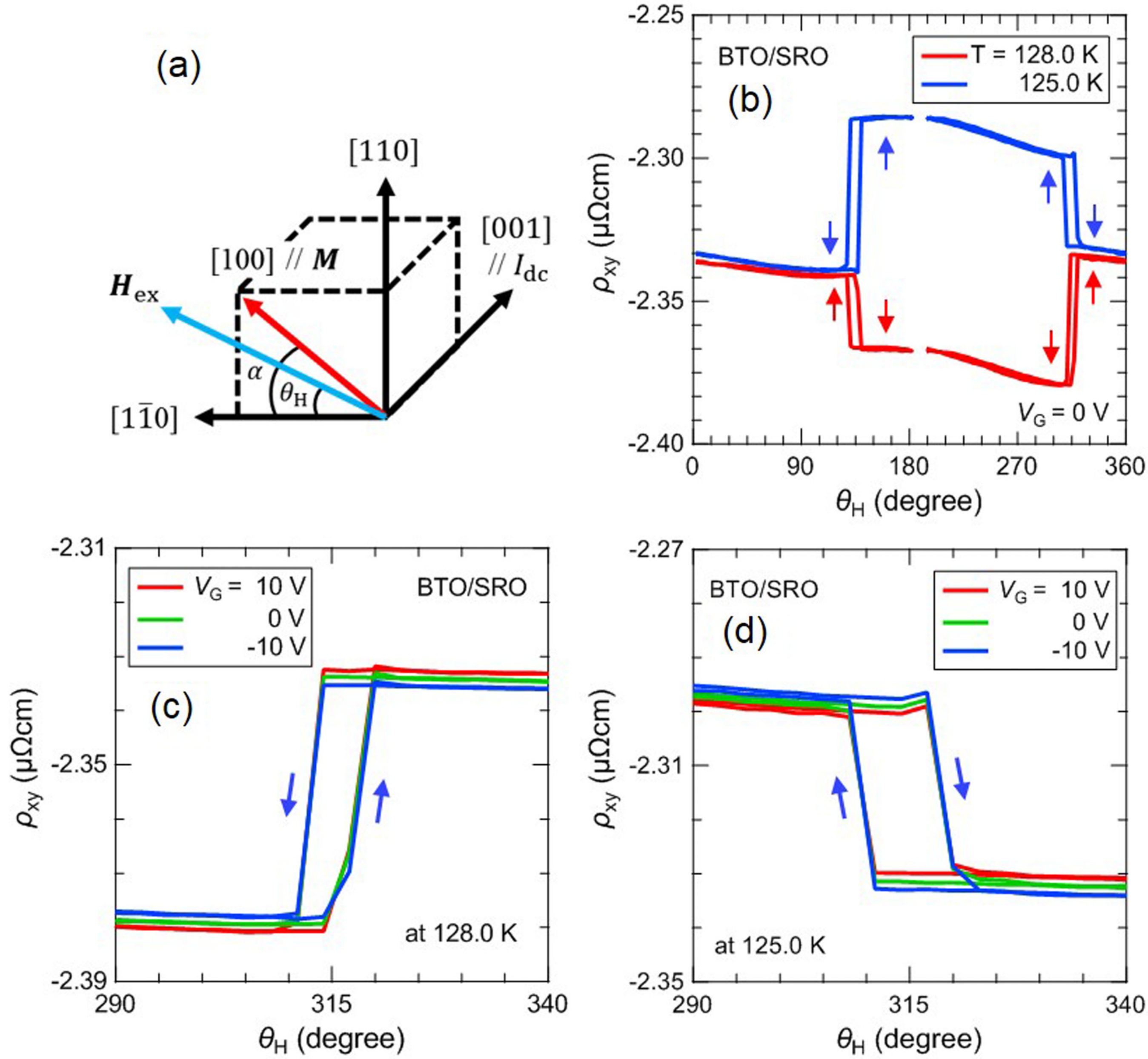

FIG. 5. Magnetic field angle θ_H dependence of the Hall resistivity ρ_{xy} for the BTO/SRO channel. (a) Measurement configurations. (b) θ_H dependence of ρ_{xy} under $V_G = 0$ V at 128.0 K (red) and 125.0 K (blue). (c), (d) θ_H dependence of ρ_{xy} under $V_G = +10$ V (red), 0 V (green), and -10 V (blue). The curves were recorded at (c) 128.0 K and (d) 125.0 K. In (b), (c), and (d), the arrows indicate the magnetic field rotation direction (clockwise and counterclockwise).

field-induced modulations on σ_{AHE} in the SRO thin films [25]. It was shown that electric-double-layer gating into the 5-monolayer-thick SRO films resulted in modulations in both ρ_{xx} and σ_{AHE}, associated with large changes in the sheet carrier concentration with an order of 10^{14} cm^{-2} (that corresponds to $\sim 10^{21}$ cm^{-3} carrier concentration). This large change in the carrier concentration and ρ_{xx} was thus considered to be responsible for the previously observed modulations of σ_{AHE} ($\sim \rho_{AHE}/\rho_{xx}^2$). On the other hand, our observations show that the V_G application into the channels modulates both the magnitude and sign of σ_{AHE}, which cannot be explained only by taking into account the electric-field-induced changes in ρ_{xx}. We also note that the V_G-induced changes in carrier concentration in our transistor structures are as small as $\sim 10^{18}$ cm^{-3} and the resultant changes in ρ_{xx} are $\sim$0.04%, far smaller than those seen in the previous study [25]. These results indicate that the V_G-induced change in ρ_{xx} is less significant in our observed electric-field-induced modulations of AHE in SRO and that the dominant mechanism behind the electric-field-induced effects is different from the previous study.

We also investigate how the application of V_G affects the magnetic anisotropy (or the magnetic easy axis direction) of the BTO/SRO channel layer, which would influence σ_{AHE} (or ρ_{AHE}). It has been shown that monoclinic SRO films on the $(110)_{ortho}$ GSO substrates exhibit uniaxial magnetic anisotropy with the magnetic easy axis along the $[100]_{ortho}$

direction [18]. Because of the strong magnetic anisotropy of SRO, the easy axis direction can be determined from the magnetic field angle dependence of ρ_{xy}: the magnetization does not follow directional changes of the magnetic field. When the angle between the magnetic field and magnetization is beyond 90°, magnetization reversal occurs; this event is seen as a jump in ρ_{xy}. Figure 5 shows the magnetic field angle θ_H dependence of ρ_{xy} under $V_G = +10$ V, 0 V, and -10 V. The data were obtained by measuring ρ_{xy} under a magnetic field rotated in the $(001)_{\text{ortho}}$ plane in clockwise and counterclockwise directions and at 128.0 K and 125.0 K where the sign of ρ_{AHE} is positive and negative, respectively. Under the condition of $V_G = 0$ V [Fig. 5(b)], the magnetization-reversal-induced jumps in ρ_{xy} with hysteresis in the clockwise and counterclockwise magnetic field rotations are seen every 180° in the field direction. The center of the hysteresis lies at 134° and 315° at 128.0 K and 134° and 315° at 125.0 K. This indicates that the SRO layer in the channel exhibits uniaxial magnetic anisotropy with the easy axis along the $[100]_{\text{ortho}}$ axis and the easy axis direction remains unchanged with temperature because of the magnetocrystalline effect. Importantly, as shown in Figs. 5(c)–5(d), applying V_G of either $+10$ V or -10 V results in no shift in the center position of the hysteresis, while the V_G-dependent change in the magnitude of ρ_{xy} is seen. The results indicate that the application of V_G has no or negligibly small influence on the easy axis direction of SRO, and the magnetic anisotropy plays no role in the observed electric-field-induced modulations of the AHE.

Important implications from our observations are that electrostatically accumulating and depleting electrons into SRO through the application of V_G modulate the integral of the Berry curvature over the filled electronic states. Because the multiple band crossings in SRO act as either a source or a sink of Berry curvature, the V_G-induced shift in the E_F position across such band crossings impact the AHE even though the carrier number changes associated with the E_F level shift is too small to modulate the magnetization magnitude and magnetic anisotropy. Our results indicate that the intrinsic mechanism correlated with the Berry curvature is dominant in the AHE of SRO. Finally, we discuss why the BTO capping layer on the SRO channel is necessary to observe the V_G-induced modulations of the AHE. It has been recently shown that the BTO capping layer on the SRO films grown on the GSO substrates stabilize gradual changes in the Ru-O-Ru bond angle in SRO from 168° at the SRO/GSO interface to 180° at the BTO/SRO interface along the growth direction [20]. Given that such bond angle changes closely tie with electronic structures and, as a result, their Berry curvature, it is reasonable to consider that the capping layer influences the band crossings in SRO and enhances the electric field effect on the AHE through the Berry curvature.

In summary, we show that in a transistor structure with a SRO channel capped with a BTO epitaxial layer, the AHE of the channel is electrically modulated by the application of V_G. The positive and negative application of V_G respectively increases and decreases the anomalous Hall conductivity, independently of its sign, while no V_G-induced change in the uniaxial magnetic easy axis direction is seen. These observations indicate that the observed V_G-induced modulations in the AHE do not simply originate from changes in both the magnitude of the magnetization and magnetic anisotropy. We also show that the transistor structure with the SRO channel having no cap layer exhibits no electric field modulations of the AHE. This indicates that the BTO cap layer, which modifies the Ru-O-Ru bond angles and consequently affects the band crossings around the E_F in SRO, plays a decisive role in enhancing the electric field effects on the AHE through the Berry curvature. Our results underline that the application of V_G changes the integral of the Berry curvature over the filled electronic states, modulating the AHE in SRO.

This work was partially supported by a grant from the Integrated Research Consortium on Chemical Sciences and by Grants-in-Aid for Scientific Research (No. 15H05702, No. 16H02266, No. 17H05217, No. 17H04813, No. 17H05181, and No. 16J06825) from the Ministry of Education, Culture, Sports, Science, and Technology (MEXT) of Japan. The work was also supported by the Japan Society for the Promotion of Science (JSPS) Core-to-Core Program (A) and Advanced Research Networks and the Cooperative Research Project Program of the Research Institute of Electrical Communication, Tohoku University.

[1] D. Xiao, M.-C. Chang, and Q. Niu, Rev. Mod. Phys. **82**, 1959 (2010).
[2] N. Nagaosa, J. Sinova, S. Onoda, A. H. MacDonald, and N. P. Ong, Rev. Mod. Phys. **82**, 1539 (2010).
[3] T. Jungwirth, Q. Niu, and A. H. MacDonald, Phys. Rev. Lett. **88**, 207208 (2002).
[4] Y. Yao, L. Kleinman, A. H. MacDonald, J. Sinova, T. Jungwirth, D.-S. Wang, E. Wang, and Q. Niu, Phys. Rev. Lett. **92**, 037204 (2004).
[5] J. Ye, Y. B. Kim, A. J. Millis, B. I. Shraiman, P. Majumdar, and Z. Tešanović, Phys. Rev. Lett. **83**, 3737 (1999).
[6] Y. Taguchi, Y. Oohara, H. Yoshizawa, N. Nagaosa, and Y. Tokura, Science **291**, 2573 (2001).
[7] S. Nakatsuji, N. Kiyohara, and T. Higo, Nature (London) **527**, 212 (2015).
[8] T. Suzuki, R. Chisnell, A. Devarakonda, Y. T. Liu, W. Feng, D. Xiao, J. W. Lynn, and J. G. Checkelsky, Nat. Phys. **12**, 1119 (2016).
[9] A. Neubauer, C. Pfleiderer, B. Binz, A. Rosch, R. Ritz, P. G. Niklowitz, and P. Böni, Phys. Rev. Lett. **102**, 186602 (2009).
[10] P. Bruno, V. K. Dugaev, and M. Taillefumier, Phys. Rev. Lett. **93**, 096806 (2004).
[11] G. Koster, L. Klein, W. Siemons, G. Rijnders, J. S. Dodge, C.-B. Eom, D. H. A. Blank, and M. R. Beasley, Rev. Mod. Phys. **84**, 253 (2012).
[12] L. Si, O. Janson, G. Li, Z. Zhong, Z. Liao, G. Koster, and K. Held, Phys. Rev. Lett. **119**, 026402 (2017).
[13] D. Kan, R. Aso, R. Sato, M. Haruta, H. Kurata, and Y. Shimakawa, Nat. Mater. **15**, 432 (2016).

[14] Z. Fang, N. Nagaosa, K. S. Takahashi, A. Asamitsu, R. Mathieu, T. Ogasawara, H. Yamada, M. Kawasaki, Y. Tokura, and K. Terakura, Science **302**, 92 (2003).
[15] M. Izumi, K. Nakazawa, Y. Bando, Y. Yoneda, and H. Terauchi, J. Phys. Soc. Jpn. **66**, 3893 (1997).
[16] M. Onoda and N. Nagaosa, J. Phys. Soc. Jpn. **71**, 19 (2002).
[17] Y. Kats, I. Genish, L. Klein, J. W. Reiner, and M. R. Beasley, Phys. Rev. B **70**, 180407 (2004).
[18] N. Haham, Y. Shperber, M. Schultz, N. Naftalis, E. Shimshoni, J. W. Reiner, and L. Klein, Phys. Rev. B **84**, 174439 (2011).
[19] See Supplemental Material at http://link.aps.org/supplemental/10.1103/PhysRevB.96.214422 for x-ray reciprocal space mappings for the BTO/SRO/GSO heterostructure.
[20] D. Kan, R. Aso, H. Kurata, and Y. Shimakawa, APL Mater. **3**, 062302 (2015).
[21] D. Kan, R. Aso, H. Kurata, and Y. Shimakawa, Adv. Funct. Mater. **23**, 1129 (2013).
[22] See Supplemental Material at http://link.aps.org/supplemental/10.1103/PhysRevB.96.214422 for the temperature dependence of the anomalous Hall conductivity σ_{AHE} for the BTO/SRO and SRO channels in the fabricated transistor structures under $V_G = 0$ V.
[23] See Supplemental Material at http://link.aps.org/supplemental/10.1103/PhysRevB.96.214422 for the V_G dependence of the electrical resistivity ρ_{xx} for the transistor structures with the BTO/SRO channel.
[24] D. A. Tenne, P. Turner, J. D. Schmidt, M. Biegalski, Y. L. Li, L. Q. Chen, A. Soukiassian, S. Trolier-McKinstry, D. G. Schlom, X. X. Xi, D. D. Fong, P. H. Fuoss, J. A. Eastman, G. B. Stephenson, C. Thompson, and S. K. Streiffer, Phys. Rev. Lett. **103**, 177601 (2009).
[25] S. Shimizu, K. S. Takahashi, M. Kubota, M. Kawasaki, Y. Tokura, and Y. Iwasa, Appl. Phys. Lett. **105**, 163509 (2014).
[26] D. Chiba, S. Fukami, K. Shimamura, N. Ishiwata, K. Kobayashi, and T. Ono, Nat. Mater. **10**, 853 (2011).
[27] C. Bi, Y. Liu, T. Newhouse-Illige, M. Xu, M. Rosales, J. W. Freeland, O. Mryasov, S. Zhang, S. G. E. te Velthuis, and W. G. Wang, Phys. Rev. Lett. **113**, 267202 (2014).
[28] K. Yamada, H. Kakizakai, K. Shimanura, M. Kawaguchi, S. Fukami, N. Ishiwata, D. Chiba, and T. Ono, Appl. Phys. Express **6**, 073004 (2013).
[29] G. Cao, S. McCall, M. Shepard, J. E. Crow, and R. P. Guertin, Phys. Rev. B **56**, 321 (1997).